The Sources of Lead Pollution in a Tropical Soil Chronosequence Based on Lead Isotope

Jianwu LI (jameslee@zafu.edu.cn)
Zhejiang A and F University
Jinlin Yang
Institute of Soil Science, Chinese Academy of Sciences
Ganlin Zhang
Institute of Soil Science, Chinese Academy of Sciences

Research Article

Keywords: Pb isotope, anthropogenic source, soil chronosequence, Hainan Island

Posted Date: June 17th, 2021

DOI: https://doi.org/10.21203/rs.3.rs-605527/v1

The sources of lead pollution in a tropical soil chronosequence based on lead isotope

Jianwu Li[1,2*] · Jinlin Yang[2] · Ganlin Zhang[2*]

[1] Key Laboratory of Soil Contamination Bioremediation of Zhejiang Province, Zhejiang A & F University, Hangzhou 311300, China

[2] State Key Laboratory of Soil and Sustainable Agriculture, Institute of Soil Science, Chinese Academy of Sciences, Nanjing 210008, China

*Corresponding authors.

**Correspondence to: Key Laboratory of Soil Contamination Bioremediation of Zhejiang Province, Zhejiang A & Forestry University, Hangzhou 311300, China.

E-mail addresses: jameslee@zafu.edu.cn (**J. Li**); 80834026@qq.com (**G. Zhang**).

Abstract

Soil is important contributor to global biogeochemical cycles and often receives anthropogenic Pb contamination. Hainan soil chronosequence developed on basalt had provided a good opportunity to identify and quantify the relative contributions of Pb sources in remote tropical areas. The results revealed that Pb concentrations and isotopic ratios of the soils were clearly affected by anthropogenic source. The Pb concentrations and percentage changes of Pb/Th ratios showed significantly Pb enrichment. The low $^{206}Pb/^{207}Pb$ values of upper soils indicated a significant addition of extraneous Pb, whereas deeper soils showed a dominantly basaltic source. The $^{208}Pb/^{206}Pb$ vs. $^{206}Pb/^{207}Pb$ diagram of soils clearly indicated inputs of parent material and anthropogenic Pb sources. We also calculated the mass fractions of anthropogenic-derived Pb ($f^{Pb}_{\text{anthropogenic}}$) based on isotope mass balance. The $f^{Pb}_{\text{anthropogenic}}$ values showed a generally decreasing trend with soil depth, implying a significant addition of anthropogenic Pb in top soils. The contribution of anthropogenic Pb in Hainan soil chronosequence highlighted the significance of anthropogenic contamination to soils globally.

Key words Pb isotope · anthropogenic source · soil chronosequence · Hainan Island

Introduction

Soil is an important contributor to global biogeochemical cycles and has played an important role in the ecosystem (Brantley et al., 2007; Ryu et al., 2020; Vogel et al., 2021). In recent decades, rapid industrialization and urbanization have introduced

great amount of contaminants, including heavy metals, from various sources into soils (Oluyemi et al., 2008; Awokunmi et al., 2010; Chai et al., 2015; Adedeji et al., 2020). Heavy metals are major contaminants in the soil environment (Peng et al., 2019; Li et al., 2020). They are resistant to biodegradation, making their accumulation in the soil environment extremely persistent (Bolan et al., 2014). Lead (Pb) is a natural constituent of the earth's crust and is commonly found in soils, plants and water (Lei et al., 2016). Pb is an especially poisonous element and is one of the most widely studied metals in environmental sciences (Zahran et al., 2009). Consumption of Pb even at very low concentrations can cause diseases of nervous, digestive and reproductive systems, and do great harms to human health (Zhang et al., 2008). Emissions of Pb have been significantly enhanced by various anthropogenic activities (Mukai et al., 2001). Thus, Pb contamination in soils environment has become an important issue for many countries and causes both human health and environment concerns (Cheng et al., 2010; Stefanowicz et al., 2010; Ajmone-Marsan et al., 2010; Kamenov et al., 2014).

Pb isotopic fingerprinting has been introduced as an effective tracer for environment pollution (Ellam, 2010; Blichert-Toft et al., 2016; Shi et al., 2018). The isotopic signatures of Pb in different environments reflect the mixing of different sources, and source apportionment of Pb can be quantified by Pb isotopic methods (Marcantonio et al., 2000; Bird, 2011; Li et al., 2020). Pb isotopic analysis has been increasingly applied for Pb contamination studies of air (Grousset et al., 2005; Hyeong et al., 2011), soils (Wong et al., 2006), sediments (Hosono et al., 2010), and plants (Marcantonio et al., 2000; Klaminder et al., 2008). The use of lead isotopic ratios was shown useful to identify different Pb origins of urban soils in Hongkong (Ettler et al., 2004). Monna et al. (2000) developed Pb isotope ratio based on models

to calculate relative contributions of various Pb sources in sediments. Thus, Pb isotopes have been proven to be valuable tracers for understanding anthropogenic lead pools and earth surface processes related to regolith development (Blichert-Toft et al., 2016; Jeon et al., 2020).

In different environments, soils are often receiving Pb from different sources (Zhang et al., 2007a; Li et al., 2011; Kapusta et al., 2015). In urban and rural areas, the sources of lead include not only anthropogenic sources, but also natural sources, such as rock weathering (Monastra et al., 2004; Li et al., 2020). Although Hainan Island is located in one of the relative clean and remote areas in China, soils may have been contaminated by anthropogenic Pb. We established a soil chronosequence developed on basalt, with a strong contrast of Pb isotopic ratios between bedrock (i.e., basalts) and anthropogenic Pb sources. This may provide an excellent opportunity to study the relative contributions of various Pb sources in rural soils. Therefore, the main objectives of this study were: (1) to investigate Pb contamination of rural soils in Hainan Island, (2) to examine the isotopic ratio of Pb and identify possible sources of the contaminant in soils, and (3) to estimate relative contributions of natural and anthropogenic Pb sources of soil chronosequence in order to reveal the effect of different soil horizons and development stage on Pb contributions.

Materials and methods

Study area and pedon description

Soil chronosequence is often used to illustrate soil genesis, which minimizes variation in many variables that can influence soil development and then allows a stronger focus on specific soil forming factors (Vidic and Lobnic, 1997; Ryu et al., 2020). Hainan Island is the second largest island in China, located in the north of South

China Sea. It is one of the largest areas of Quaternary basalts in China (Fig.1). Hainan Island is located in the tropical area with superior hydrothermal conditions, which has unique chemical weathering and soil forming conditions that obviously different from the temperate areas (Zhang et al., 2007b). It has a mean temperature of 23-24ºC and a mean annual precipitation of 1400 to 1800 mm. Meanwhile, the types of parent rocks (basalt) were very homogeneous and the differences of climate, topography and vegetation were small in Hainan Island. Thus, these homogeneous soil forming factors in Hainan Island provided favorable conditions for us to study the geochemistry of soil chronosequence in tropics.

Three Soil profiles were developed on the basalts that range in age: 180 ka (HB12), 420 ka (HB10) and 2300 ka (HB06), which was determined using K-Ar chronology. Thus, we selected them to establish a soil chronosequence. The sites were minimally eroded gently sloping shield volcano surfaces. The soils support forests that were dominated by *Eucalyptus* and *Casuarinas*. Soil pits were hand-dug, described by genetic horizon to fresh rock, and channel sampled to form an integrated homogenous unit for each horizon. The soils were classified as Primosols to Ferralsols (Chinese Soil Taxonomy (CST), 2001), which were equivalent to Entisols to Oxisols (Table 1) according to Soil Survey Staff (2014).

Laboratory analyses and calculations

Soil samples were air-dried, crushed using a wooden pestle and mortar, and then passed through a 2 mm nylon sieve. According to the different requirements of chemical analysis items, soil samples were further milled to pass the different sieves. The soil pH, soil bulk density, soil organic matter (SOM) and cation exchange capacity (CEC) were measured by methods of Lu (1999). The prepared samples

(0.149 mm, 500 mg) were weighed into a disposable graphite crucible with 700 mg of flux (1:1 mix of Li-metaborate and Li-tetraborate) and fused for 30 min in a 1000°C muffle furnace (Li et al., 2014). Then fused samples were dissolved in a solution (10% HNO_3 + 1% HF) and determined the Pb La and Th concentrations of the soils at Nanjing University using a JY 38S (JION YVON, France) single channel scanning plasma spectrometer. The standard reference materials were GSR-3, GXR-5 and GXR-6. Analytical uncertainties were less than ±2% for the trace elements.

The Pb isotopes were measured on a GV Isoprobe-T thermal ionization mass spectrometer (TIMS) at the Kay Laboratory of Crust-Mantle Materials and Environments in the Institute of Geochemistry and the methodology of Pb isotopes was described in Zhang et al. (2007a). The relative standard deviations (RSD) of 10 replicate readings of samples were generally better than 1% for $^{207}Pb/^{206}Pb$ and 0.6% for $^{208}Pb/^{206}Pb$. The average of measured $^{207}Pb/^{206}Pb$ and $^{208}Pb/^{206}Pb$ of NIST 981 were 0.9147±0.0084 and 2.1681±0.0099 as the certified values of 0.9147 and 2.1683, respectively.

One approach to determine chemical losses during weathering of primary minerals was to determine the ratio of chemical concentration in the weathered mineral to the corresponding concentration in the parent mineral. We use Th as the immobile index element for mass balance calculations in this study because Li et al. (2014) showed that Th is the least mobile elements in soils developed on basalt. The percent change in the ratio relative to the ratio in the parent sample is then defined according to Nesbitt and Markovics (1997) as:

$$\%\ \text{change of ratios} = 100 \times [(R_i - R_p)/R_p] \quad (1)$$

where R_i and R_p represent the ratio of element to a conservative element in weathered samples and fresh basalt, respectively.

We calculated the percentage contribution of anthropogenic and natural Pb sources to total Pb in soils based on isotope mass balance (Li et al., 2011). Given the Pb isotope ratios of natural source (i.e., basalts) ($^{206}Pb/^{207}Pb$=1.196), and average anthropogenic source end member ($^{206}Pb/^{207}Pb$=1.162; Komárek et al., 2008).

$$f_{\text{anthropogenic}}^{Pb} = \frac{R_{Pb}^{soil} - R_{Pb}^{basalt}}{R_{Pb}^{\text{anthropogenic}} - R_{Pb}^{basalt}} \quad (2)$$

Where $f_{\text{anthropogenic}}^{Pb}$ represented the percentage contribution of anthropogenic Pb source in soils, and the R_{Pb}^{soil}, $R_{Pb}^{\text{anthropogenic}}$ and R_{Pb}^{basalt} are the Pb isotope ratios of soils, anthropogenic-derived and basalts-derived, respectively.

Results

Physicochemical data in soils of Hainan Island

Descriptions and selected physicochemical characteristics of soils were shown in Table 1. The pH values ranged from 4.58 to 6.07, showing notable acid in all soil samples. The sand content showed an increasing trend with depth for each soil profile. The bulk density was clearly lower in A horizon than in C horizon for each soil profile. The soil organic matter (SOM) showed a decreasing trend with depth, and the cation exchange capacity (CEC) varied from 3.6 $cmol^{+}\ kg^{-1}$to 23.6 $cmol^{+}\ kg^{-1}$ in Hainan soils. It is worth noting that the pH, SOM and CEC values all showed a significantly decreasing trend with soil ages for the HB12, HB10 and HB06 profiles.

Pb elemental and isotopic characteristics of soils

The concentrations of Th, La and Pb for the fresh basalt were 1.76 $mg\,kg^{-1}$, 11.7 $mg\,kg^{-1}$ and 2.31 $mg\,kg^{-1}$ in this study, respectively. The Pb concentrations ranged from 9.1 to 70.5 $mg\,kg^{-1}$ (Table 2). It's important that the Pb concentrations especially for the top

soils (0~30 cm) were significantly higher than the fresh basalt. The percentage changes of Pb/Th ratios relative to the fresh basalt were calculated according to equation (1) to estimate mobility and losses of elements. The changes of La/Th ratio were negative (Table 2). The changes of Pb/Th ratios of soils were all positive, with maximum values up to 205%, 820% and 271% in HB12, HB10 and HB06, respectively.

The $^{206}Pb/^{207}Pb$ and $^{208}Pb/^{206}Pb$ value of the fresh basalt were 1.196 and 2.076, respectively. The $^{206}Pb/^{204}Pb$, $^{208}Pb/^{206}Pb$ and $^{206}Pb/^{207}Pb$ ratios of Hainan soils were shown in Table 2. One the one hand, the low $^{206}Pb/^{207}Pb$ ratios (~1.17) were found in top soils, showing great distinct with their parent rocks. The Pb isotopic ratios of soils in top soils ($^{208}Pb/^{206}Pb$=2.105) were also far from those values of their parent rocks ($^{208}Pb/^{206}Pb$=2.076), indicating anthropogenic Pb addition in Hainan soils. On the other hand, the $^{206}Pb/^{207}Pb$ ratios of soils had an increasing trend with the soil depth. The $^{206}Pb/^{207}Pb$ ratios ranged from 1.180 to 1.192, 1.171 to 1.181 and 1.179 to 1.196 in the HB12, HB10 and HB 06 profiles, respectively (Fig. 2).

Discussion

Both the Pb concentrations and percentage changes of Pb/Th ratios implied significantly enrichment of Pb in Hainan soil chronosequence. Thus, except for being residue of the parent rock, there may exits extraneous inputs of Pb. Several fold increases in lead concentrations in top soils suggested that soils have been significantly impacted by anthropogenic Pb (Table 2). The $^{206}Pb/^{207}Pb$ ratios in the lower horizon were close to the ratio of their parent rocks, indicating Pb source of basaltic weathering; while the $^{206}Pb/^{207}Pb$ ratios of soils in top soils were lower than these parent rocks, implying contamination in soils (Table 2). Since anthropogenic Pb

usually has a lower $^{206}Pb/^{207}Pb$ ratio than the naturally derived Pb (Bird, 2011), the differences of $^{206}Pb/^{207}Pb$ ratios between soils (1.176~) and their parent rocks (1.196) suggested that Pb sources with lower $^{206}Pb/^{207}Pb$ values must have been mixed into the soils. Cheng et al. (2010) also had reported conspicuous lead pollution in China. So these lower $^{206}Pb/^{207}Pb$ values, especially in the top soils of Hainan Island, south China, may indicate remarkably input of anthropogenic Pb in soils. Interestingly, there was a significant negative correlation between the isotopic ratios and concentration of Pb in soil profiles (Fig. 2). Analysis of Pb concentration and $^{206}Pb/^{207}Pb$ data shows a correlation coefficient of -0.899, -0.742 and -0.735 in the HB12, HB10 and HB06 soil profiles. The significantly negative correlation between Pb content and isotopic ratios can also be strongly demonstrated a significant addition of extraneous anthropogenic Pb (Monastra et al., 2004).

Anthropogenic Pb includes different sources, such as coal mines, gasoline. It is believed that coal burning has an impact on aerosol Pb isotope ratios. The lower $^{206}Pb/^{207}Pb$ value in soil samples might have partially resulted from the use of coal burning, since $^{206}Pb/^{207}Pb$ mostly varied from 1.14 to 1.18 in the fly ash in China (Mukai et al., 2001). Moreover, petroleum usage is another possible source with low $^{206}Pb/^{207}Pb$ (Komárek et al., 2008; Kamenov et al., 2014). As a result, we take the mean values of Asian anthropogenic Pb isotopic ratios ($^{206}Pb/^{207}Pb$=1.162, $^{208}Pb/^{206}Pb$ =2.119) as anthropogenic sources in Hainan soils. The $^{208}Pb/^{206}Pb$ vs. $^{206}Pb/^{207}Pb$ diagram of soil samples (Fig. 3) suggests that a multi-component mixing with two Pb sources. Thus, Hainan soils chronosequence contain a mixture of material derived from *in situ* weathering of parent material plus anthropogenic Pb sources inputs.

The contributions of anthropogenic and basalt Pb sources were calculated according to equation (2) and showed in Fig. 4. Mass fraction of Anthropogenic Pb

for deeper saprolite samples were low, indicating dominance of lava-derived Pb; while the mass fraction for top soils were high, with maximum values up to 74.10%, 48.65% and 46.68% in HB12, HB10 and HB06 profile, respectively. These results demonstrate that Hainan soils were influenced by anthropogenic Pb sources near the soil surface (Hosono et al., 2010).

The average contributions of anthropogenic Pb were 22%, 66% and 32% in HB06, HB10 and HB12 soil profiles, respectively. For the old soils (2300 ka), there were much more leaching losses of soluble elements, leading to relative enrichment of lava-derived Pb. So the relative contributions of anthropogenic Pb were lower than those of younger soils (Fig. 4). The significantly lower values of pH, SOM and CEC in the HB06 profile than those of HB12 and HB10 profiles (Table 1), may give rise to strong depletion in the old tropical soils (Li et al., 2014). In addition, the highest change of La/Th ratios indicated significant strong leaching of major element in HB06 (Table 2). The significantly leaching caused relative enrichment of lava-derived Pb and then led to relative low contributions of anthropogenic Pb. On the contrary, for the intermediate (420 ka) and the youngest (180 ka) age soils, there were lower leaching losses (Table 2) than those of HB06, resulting in sufficiently small enrichment of lava-derived Pb and relative high contributions of anthropogenic Pb. Furthermore, because the location of HB12 was closest to the sea (Qiongzhou Strait), the annual rainfall was higher than other sites (Fig. 1). This may cause much stronger leaching loss and lead to a relative low contributions of anthropogenic Pb than those of HB10. Thus, the contributions of anthropogenic Pb sources were related to the development stage of soil and the leaching intensity of local area.

Conclusions

Although Hainan Island is located in one of the relative least dusty regions in China, anthropogenic Pb still has a great impact on Hainan soils. Pb concentrations and isotopic ratios of the soils were clearly affected by anthropogenic Pb. The Pb isotopic ratios of soils in top soils were far from those values of parent rocks, indicating anthropogenic Pb addition in Hainan soils. The significantly negative correlation between Pb content and isotopic ratios in soils suggested a significant addition of anthropogenic Pb in the top horizon. The $^{208}Pb/^{206}Pb$ vs. $^{206}Pb/^{207}Pb$ diagram of soil samples indicated that Hainan soils contained a mixture of material derived from *in situ* weathering of parent material plus anthropogenic Pb sources inputs. The contributions of anthropogenic Pb sources showed an approximate increasing trend with soil depth. These results demonstrated that Hainan soils are influenced by anthropogenic Pb sources.

Acknowledgements This research was supported by the China Natural Science Foundation (No. 41877006) and Natural Science Foundation of Zhejiang province (LY21D010002). We also thank Mr. Mingkui Zhang of Zhejiang University for helpful reviews.

Conflict of interest statement On behalf of all authors, the corresponding author states that there is no conflict of interest.

References

Adedeji O, Olufunmilayo O, Oyebanji F (2020) Assessment of Traffic Related Heavy Metals Pollution of Roadside Soils in Emerging Urban Centres in Ijebu-North Area of Ogun State, Nigeria. J Appl Sci and Environ Manage 17(4):509–514

Albarede F, Desaulty AM, Blichert-Toft J (2012) A geological perspective on the use of Pb isotopes in archaeometry. Archa 54: 853–867

Ajmone MF, Biasioli M (2010) Trace elements in soils of urban areas. Water Air Soil Poll

213:121–143

Awokunmi EE, Asaolu SS, Ipinmorati KO (2010) Effect of leaching of heavy metals concentration of soil in some dumpsites. Afric J Environ Sci Tech 4(8):495

Brantley SL, Goldhaber MB, Ragnarsdottir KV (2007) Crossing disciplines and scales to understand the critical zone. Elements 3: 307–314

Bird G (2011) Provenancing anthropogenic Pb within the fluvial environment:developments and challenges in the use of Pb isotopes. Environ Int 37:802–819

Bolan N, Kunhikrishnan A, Thangarajan R, Kumpiene J, Park J, Makino T, Kirkham MB, Scheckel K (2014) Remediation of heavy metal (loid) s contaminated soils—To mobilize or to immobilize? J Hazard Mater 266:141–166

Blichert-Toft J, Delile H, Lee CT, Stos-Gale Z, Billstrom K, Andersen T, Hannu H, Albarède F (2016) Large-Scale tectonic cycles in Europe revealed by distinct Pb isotope provinces. Geochemistry 17: 3854–3864

Chinese Soil Taxonomy Research Group (CST) (2001) Chinese soil taxonomy. Science Press, Beijing, New York

Cheng HF, Hu YN (2010) Lead (Pb) isotopic fingerprinting and its applications in lead pollution studies in China: A review. Environ Pollut 158:1134–1146

Chrastný V, Vaněk A, Teper L, Cabala J, Procházka J, Pechar L, Drahota P, Penížek V, Komárek M, Novák M (2012) Geochemical position of Pb, Zn and Cd in soils near the Olkusz mine/smelter, South Poland: Effects of land use, type of contamination and distance from pollution source. Environ Monit Assess 184:2517–2536

Chai Y, Guo J, Chai S, Cai J, Xue L, Zhang Q (2015) Source identification of eight heavy metals in grassland soils by multivariate analysis from the Baicheng-Songyuan area, Jilin Province, Northeast China. Chemosphere 134:67–75

Ettler V, Milhaljevic M, Koma rek M (2004) ICP–MS measurements of lead isotopic ratios in soils heavily contaminated by lead smelting: tracing the sources of pollution. Anal Bioanal Chem 378:311–317

Ellam RM (2010) The graphical presentation of lead isotope data for environmental source apportionment. Sci Total Environ 408:3490–3492. https://doi.org/10.1016/j.scitotenv.

FAO (2006) World Reference Base for Soil Resources 2006, World Soil Resources Reports 103. FAO (Food and Agriculture Organization of the United Nations), Rome.

Grousset FE, Biscaye PE (2005) Tracing dust sources and transport patterns using Sr, Nd and Pb isotopes. Chemical Geology 222(1):149–167

Hosono T, Su CC, Okamura K, Taniguchi M (2010) Historical record of heavy metal pollution deduced by lead isotope ratios in core sediments from the Osaka Bay, Japan. J Geochem Explor 107:1–8

Hyeong K, Junguk K, Pettke T, Chan MY, Hur SD (2011) Pb, Nd and Sr isotope records of pelagic dust: Source indication versus the effects of dust extraction procedures and authigenic mineral growth. Chem Geol 286(3–4):240–251

Jeon SK, Kwon MJ, Yun ST, Yang JS, Lee S (2020) Modified approach for estimating geogenic Pb isotope ratios in soils for metal source apportionment. Environ Earth Sci 79(13):387–397

Klaminder J, Bindler R, Renberg I (2008) The biogeochemistry of atmospherically derived Pb in the boreal forest of Sweden. Appl Geochem 23:2922–2931

Komárek M, Ettler V, Chrastný V, Mihaljevic M (2008) Lead isotopes in environmental sciences: A review. Environ Int 34:562–577

Kamenov GD, Gulson BL (2014) The Pb isotopic record of historical to modern human lead exposure. Sci Total Environ 490:861–870. https://doi.org/10.1016/j.scitotenv

Kapusta P, Sobczyk Ł (2015) Effects of heavy metal pollution from mining and smelting on enchytraeid communities under different land management and soil conditions. Sci Total Environ 536:517–526

Li C, Sanchez GM, Wu ZF, Cheng J, Zhang SY, Wang Q, Li FB, Sun G, Meentemeyer RK (2020) Spatiotemporal patterns and drivers of soil contamination with heavy metals during an intensive urbanization period (1989-2018) in southern China. Environ Pollut 260:114075

Li HB, Yu S, Li GL, Deng H, Luo XS (2011) Contamination and source differentiation of Pb in park soils along an urban-rural gradient in Shanghai. Environ Pollut 159:3536–3544

Li JW, Song ZL, Zwieten LV, Ruan L, Li FL (2020) Contribution of Asian dust to soils in Southeast China estimated with Nd and Pb isotopic compositions. Acta Geochim 39(6):911–919

Li JW, Zhang GL, Gong ZT (2013) Nd isotope evidence for dust accretion to a soil chronosequence in Hainan Island. Catena 101:24–30

Li JW, Zhang GL, Gong ZT (2014) Mobilization and redistribution of elements in soils developed from extreme weathering basalt in Hainan Island. Chinese J Geochem 33(3):262–271

Li XD, Poon CS, Liu PS (2001) Heavy metal contamination of urban soils and street dusts in Hong Kong. Appl Geochem 16:1361–1368

Lei K, Giubilato E, Critto A, Pan H, Lin C (2016) Contamination and human health risk of lead in soils around lead/zinc smelting areas in China. Environ Sci Pollut Res Int 23(13):13128–13136

Lu RK (1999) Analytical Methods of Soil Agrochemistry (in Chinese). Chinese Agricultural Science and Technology Press, Beijing

Lu Y, Gong ZT, Zhang GL, Burghardt W (2003) Concentrations and chemical speciations of Cu, Zn, Pb and Cr of urban soils in Nanjing, China. Geoderma 115:101–111

Marcantonio F, Flowers GC, Templin N (2000) Lead contamination in a wetland watershed: isotopes as fingerprints of pollution. Environ Geol 39:1070–1076

Monna F, Hamer K, Lévêque J, Sauer M (2000) Pb isotopes as a reliable marker of early mining and smelting in the Northern Harz province (Lower Saxony,Germany). J. Geochem Explor 68:201–210

Monastra V, Derry LA, Chadwick OA (2004) Multiple sources of lead in soils from a Hawaiian chronosequence. Chem Geol 209:215– 231

Mukai H, Tanaka A, Fujii T, Zeng Y, Hong Y, Tang J, Guo S, Xue H, Sun Z, Zhou J, Xue D, Zhao J, Zhai G, Gu J, Zhai P (2001) Regional characteristics of sulfur and lead isotope ratios in the atmosphere at several Chinese urban sites. Environ Sci Technol 35 (6):1064–1071

Nesbitt HW, Markovics G (1997) Weathering of granodioritic crust, long-term storage of elements in weathering profiles, and petrogenesis of siliciclastic sediments. Geochim Cosmochim Ac 61:1653–1670

Oluyemi EA, Feuyit G, Oyekunle JAO, Ogunfowokan AO (2008) Seasonal variations in heavy metal concentrations in soil and some selected crops at a landfill in Nigeria. Int J Environ Sci Te 2(5):89–96

Peng JY, Li FX, Zhang JQ, Chen YN, Cao TH, Tong ZJ, Liu XP, Liang XH, Zhao X (2020) Comprehensive assessment of heavy metals pollution of farmland soil and crops in Jilin Province. Environmental Geochemistry Health 42:4369–4383

Ryu JS, Vigier N, Derry L, Chadwick OA (2020) Variations of Mg isotope geochemistry in soils over a Hawaiian 4 Myr chronosequence. Geochimica et Cosmochimica Acta 292:94–114

Stefanowicz AM, Niklińska M, Kapusta P, Szarek-Łukaszewska G (2010) Pine forest and grassland differently influence the response of soil microbial communities to metal contamination. Sci Total Environ 408(24):6134–6141

Soil Survey Staff (2014) Keys to soil taxonomy, 12th edition. United States Department of Agriculture, Natural Resources Conservation Service, Washington DC.

Shi G, Wang H, Liu E, Huang C, Zhao J, Song GZ, Liang C (2018) Sr–Nd–Pb isotope systematics of the Permian volcanic rocks in the northern margin of the Alxa Block (the Shalazhashan Belt) and comparisons with the nearby regions: Implications for a Permian rift setting? J Geodyn 115:43–56

Ukpong EC, Antigha RE, Moses EO (2013) Assessment of heavy metals content in soils and plants around waste dumpsites in Uyo Metropolis, Akwa Ibom State. Int J Eng Sci 2(7):75–86

Vidic NJ, Lobnic F (1997) Rates of soil development of the chronosequence in the Ljubljana basin, Slovenia. Geoderma 76:35–64

Vogel C, Helfenstein J, Massey MS, Sekine R, Kretzschmar R, Luo BP, Peter T, Chadwick OA, Tamburini F, Rivard C, Herzel H, Adam C, del Real AEP, Castillo-Michel H, Zuin L, Wang DN, Felix R, Lassalle-Kaiser B, Frossard E (2021) Microspectroscopy reveals dust-derived apatite grains in acidic, highly-weathered Hawaiian soils. Geoderma 381:114681

Wong JWC, Selvam A (2006) Speciation of heavy metals during co-composting of sewage sludge with lime. Chemosphere 63:980–986

Wuana RA, Okieimen FE (2011) Heavy metals in contaminated soils: A review of sources, chemistry, risks and best available strategies for remediation. ISRN Ecol:1–20

Zhang GL, Yang F, Zhao W, Zhao Y, Yang J, Gong ZT (2007a) Historical change of soil Pb content and Pb isotope signatures of the cultural layers in urban Nanjing. Catena 69:51–56

Zhang GL, Pan JH, Huang CM, Gong ZT (2007b) Geochemical features of a soil chronosequence

developed on basalt in Hainan Island, China. Revista Mexicana de Ciencias Geologicas. Mexican J Geol Sci 24:261–269

Zhang W, Feng H, Chang J, Qu J, Yu L (2008) Lead (Pb) isotopes as a tracer of Pb origin in Yangtze River intertidal zone. Chem Geol 257:257–263

Zahran S, Mielke HW, Weiler S, Berry KJ, Gonzales C (2009) Children's blood lead and standardized test performance response as indicators of neurotoxicity in metropolitan New Orleans elementary schools. Neurotoxicology 30:888–897

Table 1: Descriptions and selected physicochemical characteristics of soil profiles

Soil profiles	Age	Depth	Horizon	Color	pH	Clay	Silt	Sand	Dry bulk density	SOM	CEC
	ka	cm					%		g cm^{-3}	g kg^{-1}	$cmol^{+}$ kg^{-1}
HB12	180	0-16	A	10R2/2	6.07	30.4	54.7	9.1	0.96	68.9	23.6
		16-31	AC	10R3/2	5.99	36.7	45.0	11.9	1.02	55.6	20.5
		31-85	C	10R4/2	6.01	30.8	51.0	13.2	1.11	26.5	13.2
HB10	420	0-8	A	10R2/2	6.05	28.2	58.5	9.1	1.08	63.3	20.3
		8-15	AC	10R3/2	5.94	34.6	51.7	10.0	1.18	46.4	17.8
		15-32	C	10R4/2	5.99	28.1	52.0	14.5	1.19	32.3	15.2
HB06	2300	0-20	A	2.5YR3/6	4.58	32.9	51.3	9.9	0.99	42.7	13.6
		20-40	AB	2.5YR4/8	4.83	35.6	53.7	8.4	0.97	24.4	9.2
		40-70	B1	2.5YR4/8	5.13	34.5	54.9	9.3	1.05	14.2	7.5
		70-120	B2	2.5YR4/8	5.33	34.8	46.4	13.4	1.06	11.2	7.7
		120-200	B3	2.5YR4/8	5.24	38.2	40.8	18.1	1.06	5.8	6.4
		200-300	BC	2.5YR4/8	5.31	35.9	47.0	14.1	1.08	4.9	4.8
		300-350	C	2.5YR4/6	5.35	19.3	40.5	26.3	1.12	3.95	3.6

Table 2: Concentrations of Pb and Th, Pb/Th ratios and Pb isotopic ratios in Hainan soil chronosequence.

Soil profiles	Depth	Th	Pb	La/Th	Pb/Th[a]	$^{206}Pb/^{204}Pb$	$^{206}Pb/^{207}Pb$	$^{208}Pb/^{206}Pb$
	cm	mg kg^{-1}		%				
HB12	0-2	6.5	22.1	-64.7	159.1	18.4970	1.1826	2.0916
	2-4	4.9	18.8	-61.5	193.1	18.4394	1.1801	2.0939
	4-6	5.1	18.3	-62.8	173.8	18.4857	1.1816	2.0936
	6-8	5.0	19.7	-62.7	198.0	18.4904	1.1832	2.0910
	8-10	5.0	16.1	-61.6	145.6	18.5061	1.1837	2.0913
	10-12	4.9	16.4	-63.0	154.0	18.4909	1.1846	2.0886
	16-18	3.6	14.5	-72.7	205.5	18.5346	1.1862	2.0891
	30-60	4.6	10.8	-63.6	79.0	18.6213	1.1918	2.0841
	60-110	4.4	9.5	-50.4	63.8	18.5868	1.1913	2.0836
HB10	0-2	5.6	41.3	-58.4	460.9	18.3143	1.1716	2.1046
	2-4	5.5	34.8	-57.5	385.6	18.3273	1.1745	2.0990
	6-8	5.9	37.9	-58.7	392.1	18.3244	1.1733	2.1021
	8-10	5.8	70.5	-58.0	821.8	18.2905	1.1722	2.1026
	12-14	6.4	45.7	-59.2	447.0	18.2700	1.1708	2.1047
	16-18	5.8	29.4	-57.9	207.8	18.3188	1.1729	2.1017
	18-30	6.0	11.6	-58.2	46.0	18.4389	1.1812	2.0936
HB06	0-5	7.3	29.2	-86.1	203.7	18.4714	1.1833	2.0907
	5-10	7.3	29.8	-86.2	210.6	18.4132	1.1795	2.0954

10-15	6.7	32.8	-84.7	271.3	18.4581	1.1818	2.0933
25-30	7.1	33.0	-84.1	253.8	18.4981	1.1832	2.0925
45-50	6.9	26.3	-84.9	192.4	18.5353	1.1864	2.0878
60-80	6.8	27.0	-84.3	201.7	18.3734	1.1853	2.0938
80-100	6.8	25.4	-83.8	184.3	18.6284	1.1923	2.0804
120-140	7.7	25.7	-83.3	154.6	18.7191	1.1952	2.0812
140-170	7.3	23.6	-80.2	146.7	18.7355	1.1955	2.0792
170-200	6.8	19.4	-76.0	118.4	18.7604	1.1952	2.0800
200-300	7.4	20.4	-69.3	110.9	18.6260	1.1938	2.0799
300-350	5.0	9.1	-84.6	38.7	18.6192	1.1957	2.0765

[a] The Pb/Th ratios represent the changes of Pb/Th relative to basalt for Hainan soils, calculating according to equation (1).

Figure captions:

Fig. 1 The location of sampling sites for soil chronosequence. Study areas were typical basalt distribution area in north Hainan. After a number of soil profiles had been trial excavated, three of them were selected as the representative soil profiles of the region. They were near Haikou, Chengmai and Wenchang, respectively. Hainan soil chronosequence was composed of three soil profiles (180 ka: HB12, 420 ka: HB10 and 2300 ka: HB06), which were developed on *in situ* weathering of basalts.

Fig. 2 Lead concentration and $^{206}Pb/^{207}Pb$ ratios for soils in Hainan Island. Analysis of Pb concentration and $^{206}Pb/^{207}Pb$ data shows a correlation coefficient of -0.899, -0.742 and -0.735 in the HB12, HB10 and HB06 soil profiles, respectively.

Fig. 3 The $^{208}Pb/^{206}Pb$ vs. $^{206}Pb/^{207}Pb$ ratios diagram established for Hainan soils. The basalts and anthropogenic source represented the natural source (i.e., basalts) and anthropogenic Pb source end member, respectively. The average $^{208}Pb/^{206}Pb$ and $^{206}Pb/^{207}Pb$ ratios of anthropogenic end member are taken from Komárek et al. (2008).

Fig. 4 The contributions of anthropogenic Pb for Hainan soils. From the vertical comparison, mass fraction of anthropogenic Pb for deeper saprolite samples were low, indicating dominance of lava-derived Pb; while the mass fraction of upper layers (especially A horizon) were high (>40%), suggesting great influence of anthropogenic Pb sources near the soil surface. On the other hand, the contributions of anthropogenic Pb shows a trend of increasing first and then decreasing with the increase of soil age.

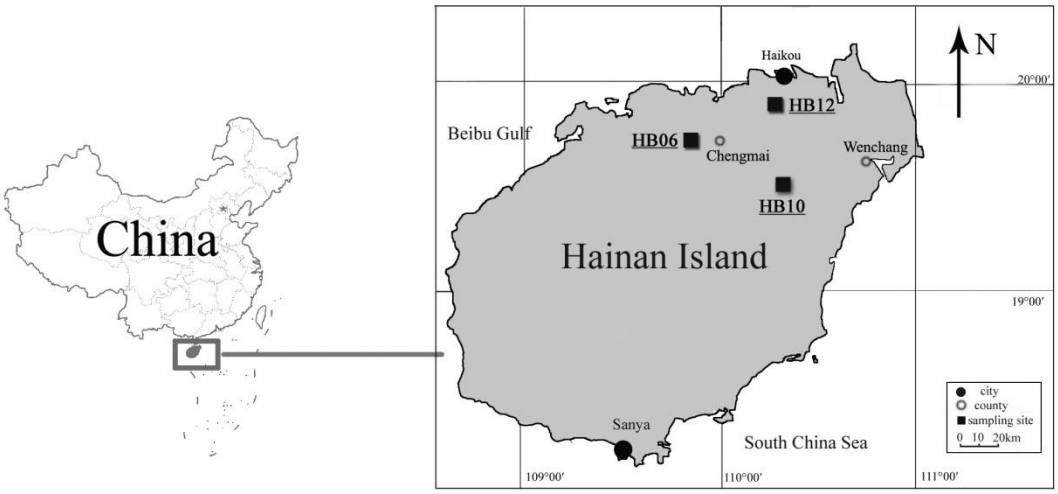
China
Haikou
HB12
Beibu Gulf
HB06
Chengmai
Wenchang
HB10
Hainan Island
Sanya
South China Sea
N
20°00′
19°00′
109°00′
110°00′
111°00′
city
county
sampling site
0 10 20km

Fig. 1

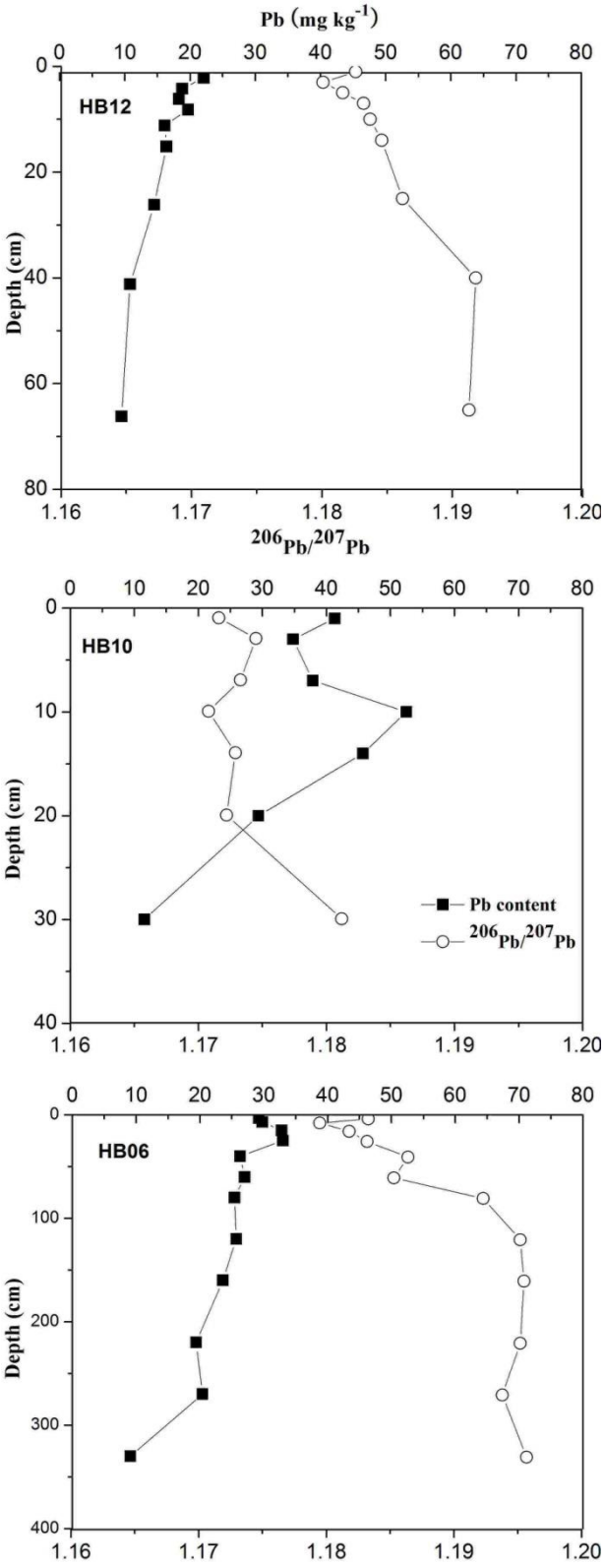
Pb (mg kg-1)
HB12
Depth (cm)
206Pb/207Pb
HB10
Pb content
206Pb/207Pb
HB06
Depth (cm)

Fig. 2

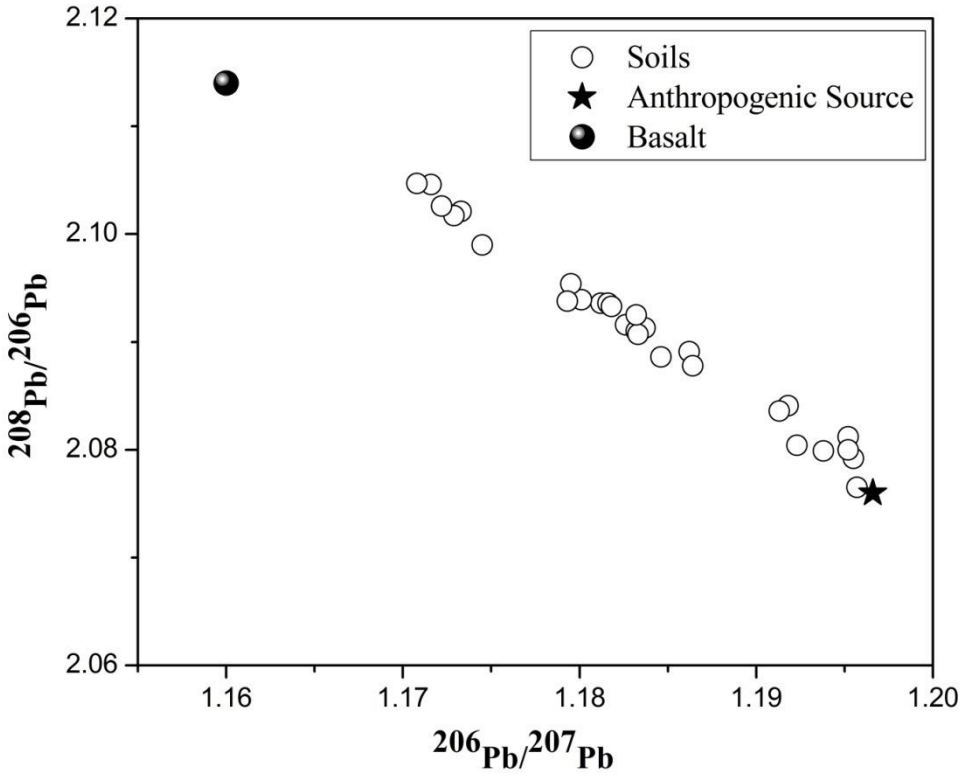
Soils
Anthropogenic Source
Basalt
2.12
2.10
2.08
2.06
1.16
1.17
1.18
1.19
1.20
208Pb/206Pb
206Pb/207Pb

Fig. 3

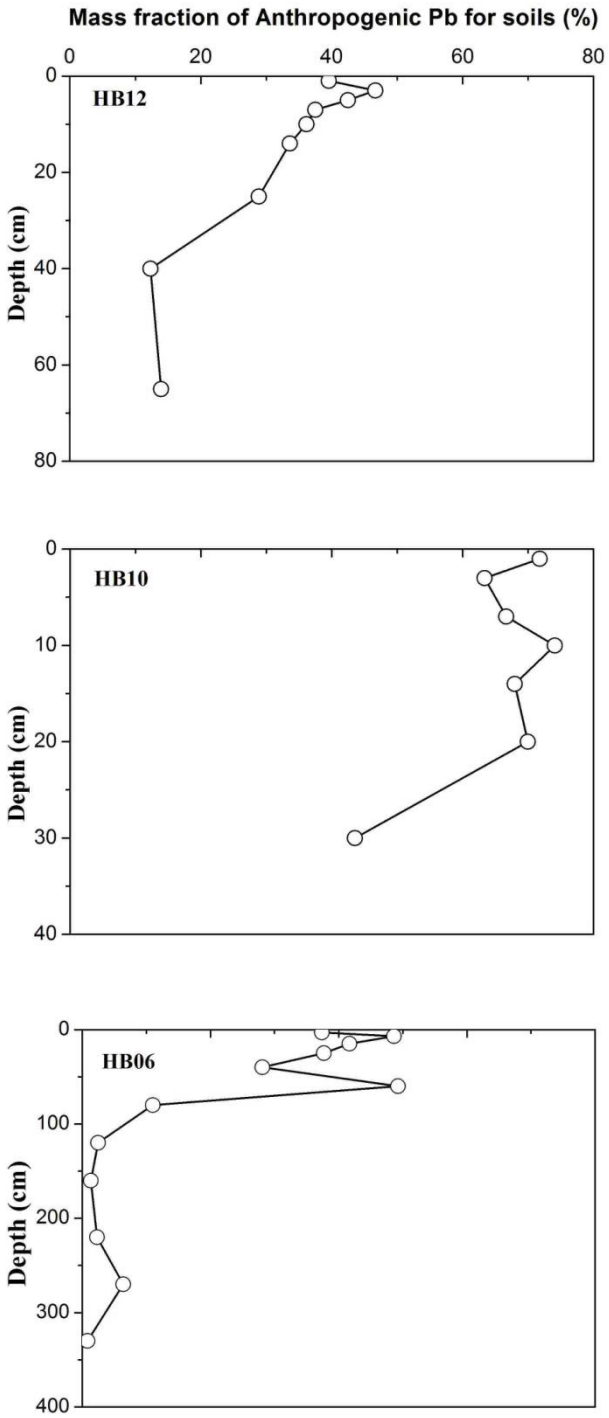
Mass fraction of Anthropogenic Pb for soils (%)
0
20
40
60
80
HB12
Depth (cm)
0
20
40
60
80
HB10
Depth (cm)
0
10
20
30
40
HB06
Depth (cm)
0
100
200
300
400

Fig. 4